JEAS

JOURNAL OF ENGINEERING
AND
APPLIED SCIENCES

Journal of Engineering and Applied Sciences, Special Issue Volume 14, Number 2, December 2018, 13-26

# MULTICHANNEL ENERGY METERS: *Multiprocessor Integration for Smart Solution*

Godwin O. Uzedhe[1] and Godswill Ofualagba[2]

Department of Electrical and Electronics Engineering, Federal University of Petroleum Resources Effurun, Delta State, NIGERIA.

uzedhe,godwin@fupre.edu.ng

**Abstract**

The number of electric energy meters (smart or otherwise) installed at consumer premises increases with urban development. These meters are developed for single supply purposes making multi-apartment homes and commercial environment to enchanter high metering space complexities. These complexities create wiring, maintenance, monitoring, and billing difficulties that results to economic challenges both for suppliers and users of electricity. This paper presents a direction towards the design and development of multichannel meters through multiprocessor integration. The approach enables multiple independent users to connect to a single supply meter and billed separately through different account entries. The integration method ensures that complex functions of measurement, data processing, communication, and load control are handled at different level of functionality in simple algorithms. The developed prototype meter maintained accuracy and consistency over time for all connected users simultaneously.  It is envisaged that its adoption for use will highly reduce metering complexities and improve economics of operation and consumption.

**Keywords:**Energy, Meter, Multi-user, Multiprocessing, Accuracy, Consistency

## 1.0 Introduction

Energy meters over the years have evolved into the digital world like every other electronic device, and have continued to experience modifications to suite usage and operational policies. These policies are constantly being modified due to social changes and technology advancement. Recently, smart energy distribution meters that enable distribution companies to monitor customer behavior in order to prevent theft are being deployed (S. Rastogi, 2016). These meters are used to bill consumers through some specified communication network, or physical data collection. The data collection processes are either by reading meter displays or through wireless non-contact communication between the meter and an electronic mobile data collection device. These methods however, are beginning to raise security concerns causing consumers to request for more policy coverage.

With the present high rate of urbanization with building congestion and the development of multi-tenanted houses, electrical power theft and meter abuse are on the increase (John Pitrus, 2013). Distribution companies are therefore deploying more technology inclined meters that can subvert criminal behaviors. This however, cannot be done in the absence of consumer concerns for the home and industrial protection. Current metering policies ran by these billing companies are yet to answer this call even with the growing rate of cybercrime (Cyril W. Drafin, 2016)(EEI-AEIC-UTC White paper, 2011)(Watts, 2003).

The space complexity of single-outlet networked energy billing meters increases tremendously with urban development. This has resulted to the development of multi-outlet connection meter through which a number of users are supplied (Chin-Shun, Chao-Yang, Feng-Sheng, & Chu-Sin, 2013.).Though these meters are smartly operated, the numerous users are seen and billed as one customer at the supplier end. The approach reduces the number of meters in use and cut down on electrical power theft as well as reduce maintenance cost but create complexities at the user end. The resultant effect of these complexities on bill payments and meter operations is none compliance to policies and regulations by users.

In this paper, a multiprocessor integration approach to multi-outlet energy meter development is used. The approach treats each connected user to a meter as a separate entity. Entities within a meter are seen as objects without any connection to each other. The objects however, share common resources such as memories, data input/output terminal and communication channels.

## 2.0 Advancement in Energy Metering Devices

Energy meters are devices that measure the amount of electrical energy consumed by other devices over time. Since their appearance in the public domain, their application has been highly challenged by users and government policies (Tomasz & Krysztof, 2013), (Anderson & Fuloria, 2014). These challenges led to constant evolution in the development of energy meters, from the early electromechanical type (Frank, Cees, & Anton) to the present chip level digital smart energy meters (Pragnya, Prasad, & Tadi, 2014), to meet the ever changing human behavior and government regulations.

The advent of digital meters has given much room to improvement on how energy is consumed at the user end (Malama, Mudenda, Ng'ombe, Makashini, & Abanda, 2014). Users can now make choices on which appliance to be powered and regulate consumption through selective management scheme (Vani & Usha, 2015). To enable seamless connectivity, manage grid parameters and check consumer behavior, smart meters are currently provided with state-of-the-art communication interface (Péter, 2011). These communication technologies are consistently opening more frontiers for electric systems management from generation to consumption (Uribe-Pérez, Hernández, David, & Angulo, 2016). However, as these technologies break through older barriers to offer new ways to electric power system management, they also come with new challenges that bear on industrial, commercial and home security (Rong Jiang_, Luo, Shen, & Xuemin, 2014) through emerging cyber-attacks. Another aspect of electric power insecurity and management problem is how the number of meters in use grows rapidly with urbanization. Electric power distribution companies are looking for ways to reduce metering and billing complexities (Marianne Hedin and Neil Strother, 2012).Meters developed so far assumes a connection point per user and focus on single-input/single-outlet meter development. Distribution authorities would suggest the use of single-input/multiple-outlet meter that can connect several users to single billing account. The method could reduce the number of meters in circulation and make for easy monitoring but create user/user tension that will result to power theft through unpaid bills. Uzedhe and Ofualagba (Uzedhe & Ofualagba, 2015), proposed the development of multichannel meter with a single billing account that is master controlled. The paper suggested that supply to any outlet is controlled internally through sub-account registration code. A master control is expected to activate compliant users or deactivate non-compliant users through a remote wireless access. This places control on human decision that can be abused through undue privileges.

## 3.0 Method

This paper utilizes a multiprocessor integration approach to meet flexible policy requirement and specifications. The approach employs different processing devices to handle separate complex functions and coordinate these functions to simplify system complexity. These complexities deals with user access control, account management system, accuracy and consistency.

The multiprocessing method handles these complexities as separate function at different levels as depicted in Fig. 1. These functions include measurement (voltage and current signal conversion, energy calculations), data processing (calibration, communication, data storage and retrieval), human-machine interface (data entry, display of information), and load control (switching and status indication). The signal conversion and energy calculation functions are handled at measurement level with a multichannel energy conversion circuit. The measurement level implement a variety of mathematical functions associated with variations in AC signals and present their digitized form for processing. The processing level uses a 16bit digital signal processing microcontroller and serves as the system's CPU to implement calibration, communication, data storage and retrieval. The processing level also interfaces the data entry and display units to form the system's human-machine interface (HMI). A load control level deals with channel switching and status indication functions. This level consist of an 8bit processor and other associated circuits that isolates and control the channel AC voltage and current to any connected load.

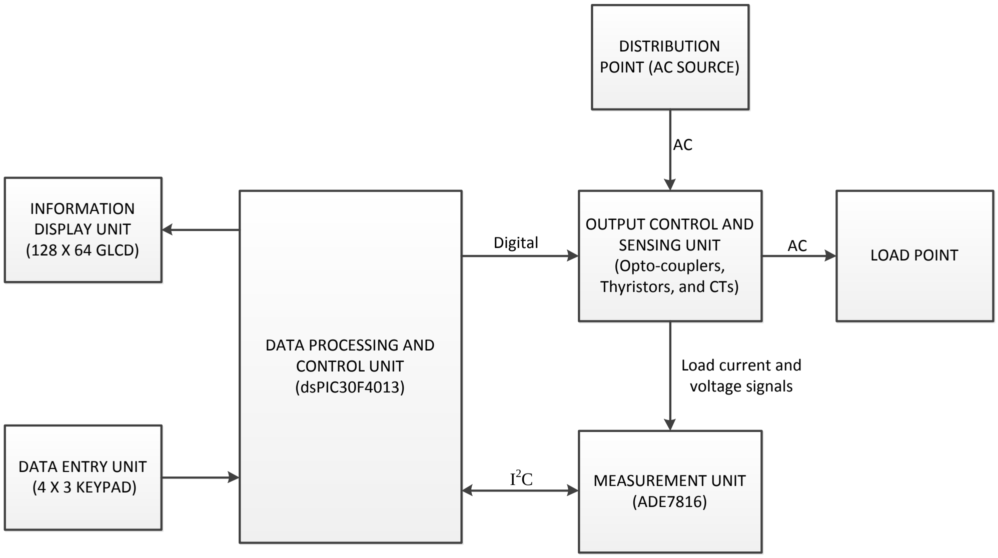

Fig. 1: Meter system block diagram

## 4.0Measurement

### *4.1 Signal Conversion and Energy Calculation*

At the center of the signal conversion and energy calculation section is the ADE7816. The ADE7816 is a multichannel energy metering IC capable of measuring line voltage, current, and calculates active energy, reactive energy, and instantaneous root mean square (rms) voltages and current. The IC uses seven sigma-delta (Σ-Δ) ADCs to provide high accuracy energy measurement. It has six current input channels and a single voltage input channel that allow multiple loads to be measured simultaneously. Each input channel supports a flexible gain stage and is suitable for use with current transformers (CTs). Rogowski coil sensors can also be used with its on-chip digital integrators.

The ADE7816 provides access to on-chip meter registers via either the Serial Peripheral Interface (SPI) or Inter-Integrated Chip ($I^2C$) interface. It equally provide power quality information, such as overcurrent, overvoltage, peak, and sag detection, via two external interrupt pins, IRQ0 and IRQ1. The ADE7816 operates on a 3.3V supply voltage packed in a 40-lead Lead Free Chip Scale Package (LFCSP) (Analog Devices, 2013).

### *4.2 Signal Conversion*

The first step in the metering system is the conversion of current drawn from each channel to its voltage equivalent and reducing the AC voltage amplitude to a level tolerable to the ADE7816.A current transformer (CT) is used as a transducer to detect any current drawn in a channel and convert same to its voltage signal equivalent using equation (1) and (2). The CSE187-L current transformer, designed to monitor low frequency signals of 50Hz to 400Hz for a current range of 0.1A to 30A, was used.

$$I_s = I_p \times \frac{N_p}{N_s} \tag{1}$$

$$V_s = I_s \times R_{DC} \tag{2}$$

Where $I_p$, $I_s$ are the primary coil current and secondary coil current. $N_p$ and $N_s$ are primary and secondary coil number of turns. $V_s$is sensed voltage and $R_{DC}$ is the burden resistance that must be connected across the secondary coil of the CT.

The ADE7816 specify a maximum input voltage of ±500mV. With the transformer ratio of the CSE187-L of 1:500, the selected burden resistance is 41Ω resulting to an output voltage of 82mV/A. At a maximum input current of 30A, the output sensed voltage is 2.46V which exceeds the maximum input voltage of the ADE7816. A voltage divider is then used according to equation (3) to produce the required voltage range of ±500mV as shown in Fig. 2.

$$V_o = \frac{V_i R_2}{R_1 + R_2} \tag{3}$$

Where,$V_i$ is maximum sensed CT output voltage and $V_o$ is required input voltage to ADE7816.

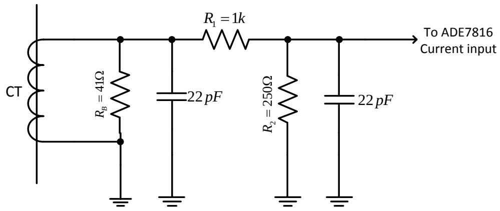

Fig. 2: Channel current sensing

The AC voltage amplitude was reduced using a series of resistors that effectively produce the required voltage level for sensing. However, ringing may occur on the AC voltage input due to load switching and feedback into the system causing the ADE7816 to freeze. This is eliminated by passing both the life and neutral lines each through a coil before the resistive network as shown in Fig. 3.

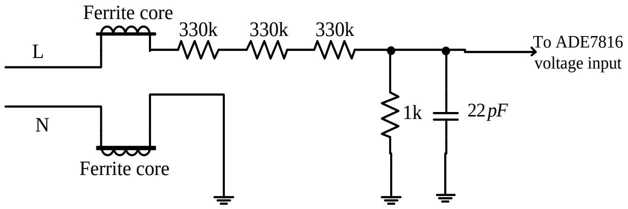

Fig. 3: Voltage sensing

The hardware circuit configuration of the signal measurement unit (Analog Devices, 2013)provides a link to all current channels, a common rms voltage signal, and digital interface to the processing unit.

### *4.3 Energy Calculation*

The instantaneous current and voltage at all harmonics with phase delays are as:

$$i(t) = \sum_{k=1}^{\infty} I_k \sqrt{2} \sin(k\omega t + \alpha_k) \tag{4}$$

$$v(t) = \sum_{k=1}^{\infty} V_k \sqrt{2} \sin(k\omega t + \beta_k) \tag{5}$$

where

$I_k$ and $V_k$ are rms voltage and current

$\alpha_k and \beta_k$ are the phase delay of each harmonics

The total active power is given by the dc component of the product of the instantaneous current and voltage as:

$$p(t) = i(t) \times v(t) = \sum_{k=1}^{\infty} I_k V_k \cos(\beta_k - \alpha_k) \tag{5}$$

With an integral number of line cycles (*n*), the average power is given equation (6) and is equal to the dc component of the instantaneous power.

$$P = \frac{1}{nT}\int_{0}^{nT} p(t)dt = \sum_{k=1}^{\infty} I_k V_k \cos(\beta_k - \alpha_k) \tag{6}$$

Where T is the line cycle period and P is the active or real power.

When in phase and filtered, resultant instantaneous current and voltage signals given as:

$$i(t) = I_{rms}\sqrt{2}\sin(\omega t) \tag{7}$$

$$v(t) = V_{rms}\sqrt{2}\sin(\omega t) \tag{8}$$

and the instantaneous power is given by the product of (7) and (8) as :

$$\begin{aligned} p(t) &= i(t)\times v(t) \\ &= I_{rms}\times V_{rms} - I_{rms}\times V_{rms}\times\cos(2\omega t) \end{aligned} \tag{9}$$

Using equations (6) and (9), the ADE7816 computes the total active power on each channel by multiplying its current and the voltage signals, and the dc component of the instantaneous power signal extracted using a low-pass filter (LPF).

Each channel's energy is calculated as integral of the power drawn over time by a connected load as:

$$E = \int_{t_1}^{t_2} p(t)dt \tag{10}$$

Where the interval $t_1 - t_2$ define the sampling intervals

The ADE7816 calculates the active energy by discretely accumulating or summing the active power over a defined sampling period *T* in discrete time *n* using equation (11).

$$E = \int_{t_1}^{t_2} p(t)dt = \lim_{T\to 0}\left[\sum_{n=0}^{\infty} p(nT)\times T\right] \tag{11}$$

The accumulated energy is stored in a 32bit register that can be read by a microcomputer through the desired communication interface.

## 5.0 Data Processing

In order to manage the operations of the ADE7816 for meter accuracy, control meter output, and allow for human-machine interface, a 16bit microcontroller, dsPIC4013, from microchip is applied. The use of the 16bit processing IC enables 16bit wide calculations and ensures proper data communication with the ADE7816 in 8bit, 16bit, 24bit and 32bit operations. The dsPIC4013 is a powerful digital signal processing controller and has numerous features such as 2kilobyte on-chip data RAM, 1Kilobyte nonvolatile data EEPROM, wide operating voltage, In-circuit serial programing, and 3wire SPI, $I^2C$, CAN communication modules (Microchip, 2010), which makes it a choice for the meter development.

### *5.1 Communication*

To enable the dsPIC4013 monitor and control the operation of the metering system, two communication processes are employed. These two processes grant access to the ADE7816 for system calibration and data acquisition, and to the output switching control. Access to the ADE7816 is through a fully licensed I$^2$C communication interface which can be enabled by holding the $\overline{SS}/HSA$ pin HIGH, and locking it in by setting Bit 1 (I2C_LOCK) of the configuration register CONFIG2 at Address 0xEC01 to 1.Communication with the ADE7816 is through Read and Write operations in 8bit, 16bit, and 32bit format.

Access to the output switching control is done using a decoded bit format, this none standard format enables independent simultaneous selection of output channels and their indicators. In this format, bits are map out as specific address input from the dsPIC4013 to the output control driver. These bits are decoded to select the required output operation at all time and are expandable to accommodate up to $2^N$, where N is the number of decoded bit pattern.

**Table 1: Decoded Bit format for output control**

| Control Code | Decoded Pattern | Operation | Status Indication |
|---|---|---|---|
| 001 | 0001 | Channel A ON | LED A ON |
| 002 | 0010 | Channel A OFF | LED A OFF |
| 003 | 0011 | Channel B ON | LED B ON |
| 004 | 0100 | Channel B OFF | LED B OFF |
| 005 | 0101 | Channel C ON | LED C ON |
| 006 | 0110 | Channel C OFF | LED C OFF |
| 007 | 0111 | Channel D ON | LED D ON |
| 008 | 1000 | Channel D OFF | LED D OFF |
| 009 | 1001 | Channel E ON | LED E ON |
| 010 | 1010 | Channel E OFF | LED E OFF |
| 011 | 1011 | Channel F ON | LED F ON |
| 012 | 1100 | Channel F OFF | LED F OFF |
| 013 | 1101 | All Channels ON | All LEDs ON |
| 013 | 1110 | All Channels OFF | All LEDs OFF |

### *5.2 Calibration*

Accuracy and consistency is a very important aspect of a metering system. The ADE7816 contains a number of registers relating to gain calibration, phase calibration, offset calibration, and other register settings. The calibration procedure includes current gain matching of all channels, phase calibration if there are power factor deviations, establishment of Wh/LSB constant, setting of active and/or reactive energy gain as required, and setting of active and reactive energy offset if meter does not meet specified accuracy at low current.

The current matching is done using:

$$IxGain = 2^{23} \times \left[ \frac{IyGain}{IxGain} - 1 \right] \tag{12}$$

Where *y* is a selected channel current against which any other channels *x* is to be matched.

With a fixed load RMS current of 5A, readings obtained and their corresponding matching current gain are given in table 2.

**Table 2: Current gain calculations**

| Channel ID | RMS Current Reading | Current Gain | Current Gain in HEX |
|---|---|---|---|
| Channel A | 370000 | 0 | 0x000000 |
| Channel B | 300000 | 1623601 | 0x18C631 |
| Channel C | 300000 | 1623601 | 0x18C631 |
| Channel D | 320000 | 1310720 | 0x140000 |
| Channel E | 320000 | 1310720 | 0x140000 |
| Channel F | 300000 | 1623601 | 0x18C631 |

The hexadecimal values are loaded into the corresponding channel current gain registers to match all channel current reading to a common value.

Phase calibration can be done by determining the phase error of each channel and calculating the Power Factor Coefficient (*PCF*) using equations (13), (14), (15) and (16)

$$Error(°C) = \tan^{-1}\left[\frac{xW\sin(\theta) - xV\cos(\theta)}{xV\sin(\theta) + xW\cos(\theta)}\right] \tag{13}$$

$$xPCF_{Fraction} = \frac{\sin(error + 3\omega) - \sin\omega}{\sin(error + 4\omega)} \tag{14}$$

If $xPCF \geq 0$, then

$$xPCF = 2^{23} \times xPCF_{Fraction} \tag{15}$$

If $xPCF < 0$, then

$$xPCF = (2^{23} + 2^{28}) \times xPCF_{Fraction} \tag{16}$$

Where, *xW* and *xV* are the active and reactive energy readings of each channel.

In order to convert energy readings to real-world values, the watt-hour per LSB(Wh/LSB) constant must first be established. This constant serves as a weighing factor of each LSB of the energy registers and can be determined using equation (17).

$$Wh/LSB = \frac{Load(W) \times Accumulation\ Time(\text{sec})}{Channel\ \text{Energy Reading} \times 3600\,\text{sec}/hr} \tag{17}$$

The active energy gain of each channel is then determined using equations (18) and (19).

$$Energy\ Gain = 2^{23} \times \left[ \frac{Expected\ \text{Energy}\ \text{Reading}}{Actual\ \text{Energy}\ \text{Reading}} - 1 \right] \tag{18}$$

$$Expected\ \text{Energy}\ \text{Reading} = \frac{Load(W) \times Accumulation\ Time(\text{sec})}{Adjusted\ Wh/LSB \times 3600\,\text{sec}/hr} \tag{19}$$

Table 3 shows energy gain calculations on a load of 105W, at an accumulation time of 8sec on a 50Hz system. The adjusted Wh/LSB value was deliberately chosen to be less than the least of the calculated Wh/LSB values to ease calculation of expected energy readings. Each channel gain is adjusted with the calculated energy gain values in their respective gain register.

Table 3: Active energy gain calculation

| Channel ID | Actual Energy Reading | Calculated Wh/LSB | Adjusted Wh/LSB | Expected Energy Reading | Energy Gain |
|---|---|---|---|---|---|
| A | 3000 | 7.8 x $10^{-5}$ | 6 x $10^{-5}$ | 3889 | 2485824 (0x25EE40) |
| B | 3100 | 7.5 x $10^{-5}$ | 6 x $10^{-5}$ | 3889 | 2135036 (0x2093FC) |
| C | 3100 | 7.5 x $10^{-5}$ | 6 x $10^{-5}$ | 3889 | 2135036 (0x2093FC) |
| D | 3400 | 6.9 x $10^{-5}$ | 6 x $10^{-5}$ | 3889 | 1206479 (0x1268CF) |
| E | 3200 | 7.3 x $10^{-5}$ | 6 x $10^{-5}$ | 3889 | 1806172 (0x1B8F5C) |
| F | 3000 | 7.8 x $10^{-5}$ | 6 x $10^{-5}$ | 3889 | 2485824 (0x25EE40) |

### *5.3 Data Storage and Retrieval*

The operation of the metering device involves the storage of energy unit loaded by a user to a given directory. These directories are memory locations in the internal 1Kilobyte nonvolatile data EEPROM of the dsPIC30F4013 microcontroller mapped to the different channels objects within the meter. This ensures that user information is not lost even if power supply to the meter is cut off. It also ensures that user data are updated at all time during consumption and credit loading.

## 6.0 Human-machine interface

The data entry and information display sections form the human-machine interface (HMI) for the metering device. The HMI provides access to the various user/service operations of the meter. The HMI used is a simple interface with a 4x3 numeric keypad and that is easily accessible to the majority of users. The use of such interface is intended to cover a wide range of users.

### *6.1 Data Entry*

The data entry unit is a 4 x 3 keypad with common key codes (1, 2, 3, 4, 5, 6, 7, 8, 9, 0, *, #), as shown in Fig. 4, that are used for operational functions. The keys are mapped out to different bit pattern that are read and decoded to their true values in software as shown in Table 5.

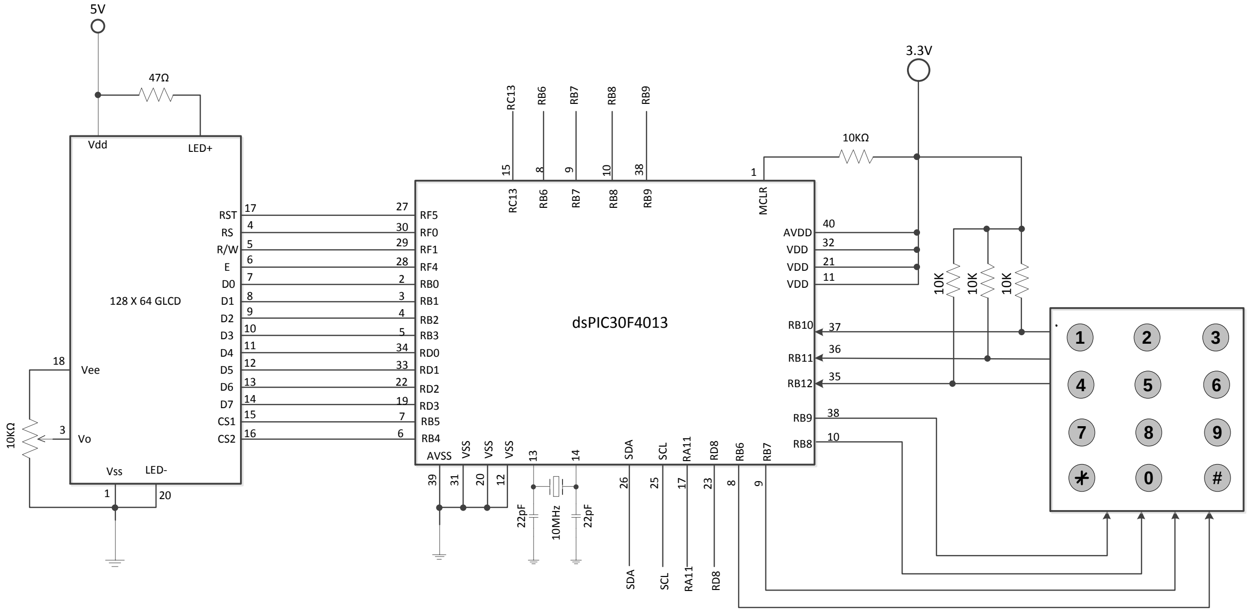

Fig. 4: HMI and data interface hardware circuit configuration

Table 5: Keypad mapping

| | Input Bit Pattern | | | | Output Bit Pattern | | | |
|---|---|---|---|---|---|---|---|---|
| Key | RB6RB7RB8RB9 | | | | RB12RB11RB10 | | | Decoded ASCII Value |
| 1 | 1 | 1 | 1 | 0 | 1 | 1 | 0 | 00110001 (031hex) |
| 2 | 1 | 1 | 1 | 0 | 1 | 0 | 1 | 00110010 (032hex) |
| 3 | 1 | 1 | 1 | 0 | 0 | 1 | 1 | 00110011 (033hex) |
| 4 | 1 | 1 | 0 | 1 | 1 | 1 | 0 | 00110100 (034hex) |
| 5 | 1 | 1 | 0 | 1 | 1 | 0 | 1 | 00110101 (035hex) |
| 6 | 1 | 1 | 0 | 1 | 0 | 1 | 1 | 00110110 (036hex) |
| 7 | 1 | 0 | 1 | 1 | 1 | 1 | 0 | 00110111 (037hex) |
| 8 | 1 | 0 | 1 | 1 | 1 | 0 | 1 | 00111000 (038hex) |
| 9 | 1 | 0 | 1 | 1 | 0 | 1 | 1 | 00111001 (039hex) |
| 0 | 0 | 1 | 1 | 1 | 1 | 1 | 0 | 00110000 (030hex) |
| * | 0 | 1 | 1 | 1 | 1 | 0 | 1 | 00101010 (02Ahex) |
| # | 0 | 1 | 1 | 1 | 0 | 1 | 1 | 00100011 (023hex) |

## 7.0 Load control (Switching and coupling)

Six independent load channels and six status indicators are required for this meter. Hence, a minimum of twelve (12) non-multiplexed output lines are required. The dsPIC30F4013 connects a PIC18F2520 through some I/O pins to implement a non-standard decoded bit format as described in Table 1. With respect to the decoded function, the PIC18F2520 control the switching and status indication of each channel. The outputs from the PIC18F2520 are coupled to the AC load with an MOC3061 opto-coupler and a BTA41/600V triac.

## 8.0 Operational and Energy acquisition Algorithms

The operation of the meter is controlled by a simple algorithm that presents the user with flexible options as shown in Fig. 5. These options enable the user to view a particular section or load energy credit data to a given user account using a specified user identification code. Each section can be exited manually by the user or automatically by a timing process. The user ID and exit process ensures privacy of users and as well prevent indiscriminate operation of the meter.

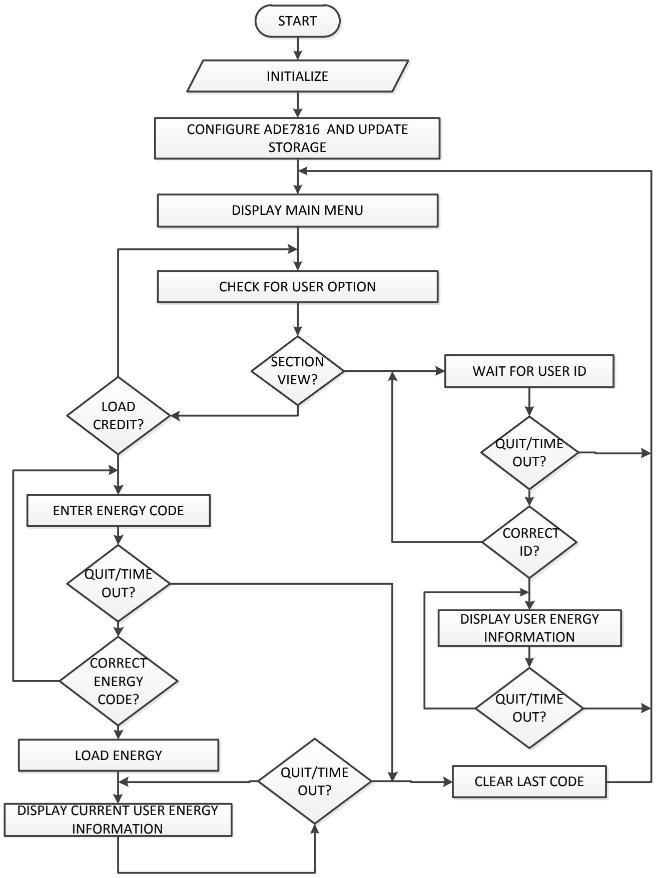

Fig. 5: Main operational algorithm

## 9.0 Results and Discussions

The developed multichannel meter prototypes shown in Fig. 6 was tested and used to power different types of loads. The results obtained indicated that energy can be supplied to homes at a reduced cost of metering with guaranteed accuracy, safety and security. A plot of energy consumed against applied load for a period of five hours (5h) as shown in Fig.7 indicates that the meter maintain the good accuracy over all channels. It also shows that multichannel energy meters can best replace single channel meters in homes and industries with independent budgets.

Figure 6: Prototype meter

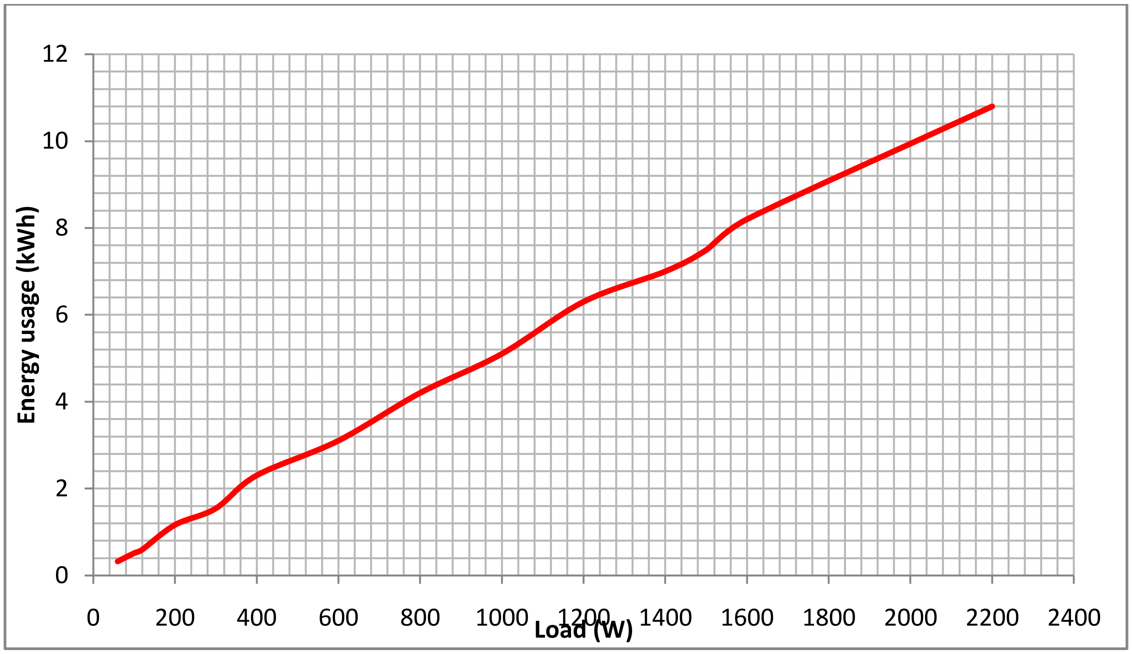

**Figure 7: Plot of load against energy consumed**

## 10.0 Conclusion

Digital technology has given room to advances in meter development. Application of single outlet meters over the years have led to metering explosion resulting to littering of multi-apartment buildings with complex wiring layout and increased energy theft threat to electric energy distribution. Electricity users in multi-apartment buildings have also finds it difficult to deal with the use of “one single-outlet meter for all”. The multichannel metering option presented in this paper has proffer solution to the myriad of problems facing electrical energy distribution in multi-apartment buildings as well as in congested areas. It also provided a new direction to smart meter development with numerous flexibilities. The method applied shows that multichannel smart meters are as consistent and accurate as their single-outlet counterparts and can even be smarter.

## Acknowledgement

We are very much grateful to the Federal University of Petroleum Resources, Effurun (FUPRE) for her technical and equipment support, and the Tertiary Education Trust Fund (TetFund) for the funding of this research work.

## References

Analog Devices. (2013). *ADE7816 Data Sheet.* Analog Devices, Inc.

Anderson, R., & Fuloria, S. (2014). *Smart Meter Security: a survey.* Cambridge University.

Chin-Shun, H., Chao-Yang, L., Feng-Sheng, H., & Chu-Sin, Y. (2013.). Meter data management system with multi-channel power supply and matrix electrical measurements. *Applied Mechanics and Materials*, 995—1001.

Cyril W. Drafin. (2016). *Cybersecurity White Paper.* MIT Energy Initiative Utility of the Future.

EEI-AEIC-UTC White paper. (2011). *Smart Meters and Smart Systems: A Metering Industry Perspective.* Washington, DC: Edison Electric Institute (EEI).

Frank, L., Cees, K., & Anton, M. (n.d.). Static Energy Meter Errors Caused by Conducted Electromagnetic Interference. *Practical Papers, Articles and Application Notes* (pp. 49—55). IEEE Electromagnetic Compatibilty Magazine.

John Pitrus. (2013). *Electric Utilities can Protect Revenue Through New Advances in Smart Meter Electronics.* Analog Devices, Inc.

Malama, A., Mudenda, P., Ng'ombe, A., Makashini, L., & Abanda, H. (2014). The Effects of the Introduction of Prepayment Meters on the Energy Usage Behaviour of Different Housing Consumer Groups in Kitwe, Zambia. *AIMS Energy*, 237-259.

Marianne Hedin and Neil Strother. (2012). Prepaid Electric Metering Hardware, Software, and Services for Prepaid Metering: Opportunities, Challenges, the Competitive Landscape and Global Market Forecasts. *Pike Research*.

Microchip. (2010). *dsPIC30F4013 Data Sheet.* Microchip Technology, Inc.

Péter, K. (2011). Smart meter based energy management system. *RE&PQJ*.

Pragnya, G., Prasad, D., & Tadi, C. S. (2014). An On Chip Design for Prepaid Electricity Billing System. *International Journal of Scientific Engineering and Technology Research*, 0212-0218 .

Rong Jiang_, R. L., Luo, J., Shen, C., & Xuemin, S. (2014). Energy-Theft Detection Issues for Advanced Metering Infrastructure in Smart Grid. *TSINGHUA SCIENCE AND TECHNOLOGY*, 105-120.

S. Rastogi, M. S. (2016). Internet of Things based Smart Electricity Meters. *International Journal of Computer Application*, 13-16.

Tomasz, Z., & Krysztof, G. (2013). Smart Metering and Data Privacy Issues. *Information systems in Management*, 239—249.

Uribe-Pérez, N., Hernández, L., David, d. l., & Angulo, I. (2016). State of the Art and Trends Review of Smart Metering in Electricity Grids. *Appl. Sci.*, 6-68.

Uzedhe, G. O., & Ofualagba, G. (2015). Multichannel Distribution Meter: A Veritable Solution in Power Distribution and Theft Prevention in Congested Environments. *Nigerian Journal of Technology (NIJOTECH)*, 844 – 850.

Vani, G., & Usha, R. (2015). Application of Smart Energy Meter in Indian Energy Context. *IOSR Journal of Electrical and Electronics Engineering (IOSR-JEEE)*, 07-13.

Watts, D. (2003). Security & Vulnerability in Electric Power System. *35th North American Power Symposium* (pp. 559-566). Missouri: University of Missouri-Rolla in Rolla.